Behavior of Columns Confined With FRP Fabrics under Repeated Lateral Loads

Hesham A. Haggag[1*], Nagy F. Hanna[1] and Ghada G. Ahmed[2]

[1]*Department of Civil Engineering, Helwan University, Elmatariah, Cairo, Egypt.*
[2]*Department of Construction Engineering, Egyptian Russian University, Badr City, Cairo, Egypt.*

Authors' contributions

This work was carried out in collaboration among all authors. All authors read and approved the final manuscript.

Article Information

Original Research Article

ABSTRACT

The axial strength of reinforced concrete columns is enhanced by wrapping them with Fiber Reinforced Polymers, FRP, fabrics. The efficiency of such enhancement is investigated for columns when they are subjected to repeated lateral loads accompanied with their axial loading. The current research presents that investigation for Glass and Carbon Fiber Reinforced Polymers (GFRP and CFRP) strengthening as well. The reduction of axial loading capacity due to repeated loads is evaluated. The number of applied FRP plies with different types (GFRP or CFRP) are considered as parameters in our study. The study is evaluated experimentally and numerically. The numerical investigation is done using ANSYS software. The experimental testing are done on five half scale reinforced concrete columns. The loads are applied into three stages. Axial load are applied on specimen in stage 1 with a value of 30% of the ultimate column capacity. In stage 2, the lateral loads are applied in repeated manner in the existence of the vertical loads. In the last stage the axial load is continued till the failure of the columns. The final axial capacities after applying the lateral action, mode of failure, crack patterns and lateral displacements are recorded. Analytical comparisons for the analyzed specimens with the experimental findings are done. It is found that the repeated lateral loads decrease the axial capacity of the columns with a ratio of about (38%-50%). The carbon fiber achieved less reduction in the column axial capacity than the glass fiber. The column confinement increases the ductility of the columns under the lateral loads.

_____

Corresponding author: Email: hahaggag@gmail.com;

1. INTRODUCTION

Confinement of columns is a way to enhance the axial capacity of concrete columns. Many of existing structures have a lack in reinforcement details to resist the seismic loads since they were built before the seismic code requirements are set. Therefore; those existing structures should be upgraded to sustain any increase in stresses due to earthquakes or any lateral loads. Numerous studies have been done about retrofitting columns against earthquakes either by traditional techniques (concrete jackets – steel jackets) [1,2,3,4,5] or by confining with Fiber Reinforced Polymer fabrics (FRP) [6-12]. S. Memon et al. [6] 2005, tested eight specimens under axial compression loads and cyclic lateral displacements. The test results showed that ductility, shear and moment capacities was enhanced by retrofitting columns with GFRP wraps, also the cyclic behavior was improved with increase the number of GFRP layers.

Stathis and Michael [7] 2003, presented an experimental study for retrofitting columns with concrete jacket and fiber wrapping to study the effect of jacketing under cyclic loading on lacking of lap splices. The test results showed that jacketing is a very effective way of enhancing the deformation capacity of columns.

Hamid Saadatmanesh et al. [8] 1997, tested four columns up to failure under cyclic loading, then columns were repaired with FRP wraps and re-tested under simulated earthquake loading. Results showed that both flexural strength and displacement ductility of repaired columns were higher than those of the original columns.

1.1 Objective

The main objective is to evaluate the reduction of the axial capacity of strengthened columns after they are subjected to repeated lateral loads. Experimental and analytical studies are carried out on columns confined with two types of FRP fabrics. The variable parameters utilized in our study are: the type of confinement material, carbon or glass FRP fabrics, and the number of the applied FRP plies: one or two.

The behaviour of such strengthening is examined through tracing the cracks' pattern, measuring the lateral displacements and the axial capacity of tested columns.The loads are applied into three stages. Axial load are applied on specimen in stage 1 with a value of 30% of the ultimate column capacity. In stage 2, the lateral loads are applied in repeated manner in the existence of the vertical loads. In the last stage the axial load is continued till the failure of the columns. Then, those columns are numerically examined using a general purpose finite element program, ANSYS. The numerical model is compared with the experimental findings.

2. EXPERIMENTAL PROGRAM

The experimental program is done on five half scale reinforced concrete columns. The specimens are investigated for the axial loading capacity after applying repeated lateral loads at the top of the columns. The columns are constructed in the RC laboratory, at Faculty of Engineering, at Matriah, Helwan University. The experimental test program was done under lateral cycles of loading and unloading with the existence of axial load. The specimens are detailed as:

- A control specimen (without wrapping).
- Two fully confined specimens with glass fiber (single and double wrapping).
- Two fully confined specimens with carbon fiber (single and double wrapping).

2.1 Description of the Tested Specimens

All columns have the same cross-sectional area of 250x250 mm, the same height of 1500 mm, the same reinforcement ratio, and the same footing dimensions. The details of the specimen reinforcement is shown in Fig. 1. Three standard cubes for each column were tested after 28 days for the material compressive strength. The average compressive strength of the cubes is 30 MPa. The columns are reinforced with vertical bars of 6T12. Closed stirrups of 5R8/m are built as shown (T and R) represent steel material with yield strength of fy=360 and 240 MPa respectively. The columns are fully wrapped with GFRP and CFRP fabrics. The specimens are divided into three categories. One column is built without fiber wrapping. This column is used as a control specimen. Two columns are built and then confined with glass FRP warping by one or two layers. Similar columns are built and then confined with carbon FRP warping by one or two layers. The details of the specimens are shown in Table 1.

2.2 Properties of the Used Materials

The used concrete mixture are designed and used for the column specimens at the faculty laboratory. Three standard cubes for each column were tested after 28 days for the material compressive strength. The average compressive strength of the cubes is 30 MPa. The columns are fabricated with main steel reinforcement bars having a yield strength of f_y=360MPa. The yield strength of the stirrups is 240 MPa. The columns are wrapped with CFRP and GFRP fabrics with physical properties as shown in Table 2. The epoxy is used as an adhesive material with properties shown in Table 3.

3. TEST SETUP

All experiments have been carried out in the Faculty of Engineering – Helwan University – Mattaria Branch. Our specimens were installed on a heavy steel frame. The footing was supported on the frame as a fixed support with four steel rods, and the top of the column was set to be free. A steel cap was placed at the top of the column in order to prevent crushing beyond the load cell. Two jacks were used: vertical jack for applying vertical axial load, and horizontal jack for applying horizontal load. Each jack

applied its load on a load cell which can read the load value. Fig. 2 shows the test set-up.

3.1 Measurements

Measuring the horizontal displacement: Three Linear Voltage Displacement Transducers, LVDTs, are placed along the column height at Levels (0.25, 0.5, and 0.75) of the column height. Also, additional LVDT is placed at the level of acting of the horizontal load cell as shown in Fig. 2.

Measuring the loads: The vertical and the horizontal loads are measured using load cells.

Measuring the strains in the reinforcement bars: Electrical strain gauges are attached to the vertical reinforcement bars to measure their strains. The strain gauges type has gauge lengths of 6mm, the gauge resistance is 120.3 ± 0.50 ohm, and the gauge factor is 2.12±1.0%. For each column four strain gauges were installed. Two of them were placed in the column's reinforcement just above the footing by 5 cm in the vertical direction whereas the other two gauges were placed with 20 cm in above on the same bar as shown in Fig. 3. The strain gauges are connected to a strain meter device with accuracy of 1×10^{-6} as shown in Fig. 4.
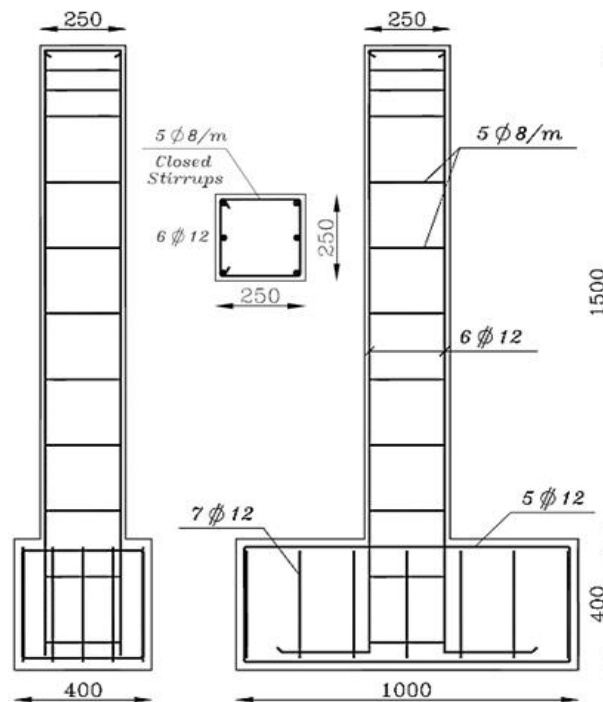

Fig. 1. Dimension of the specimens and reinforcement details

3.2 Testing Procedure

The testing is done in according to the following steps:

1. The vertical load is applied gradually up to 30% of the ultimate axial strength of the column cross section. Those values are calculated for each specimen considering the confinement effect. That load is kept constant during step 2 of the test.
2. The horizontal load is applied after step 1 and increased gradually in cyclic mater. In each cycle the horizontal load reaches a certain value and then it is released to return to the zero value. The maximum values for the cycles are set to (0.5, 1, 2, 4, 8 and 16) tons. Fig. 5 shows the planed repeating loading history. The horizontal loads is applied till the loading degradation (failure condition).
3. In this step the horizontal jack is released from the specimens and the axial load is increased gradually up to failure to investigate the maximum axial loading capacity after the failure due to the repeated lateral loads.

The results are recorded during the test and several items are recorded: (1) lateral and axial loads at the failure stages, (2) lateral load–displacement curve, (3) failure modes, (4) crack patterns, and (5) deformed shape.

4. EXPERIMENTAL RESULTS

The results of each step of testing are recorded. The cracking pattern for each specimen is documented for step 2,3 of loading. In addition, the relation of the load-horizontal displacement are constructed for each specimens.

4.1 Cracking Pattern

The crack pattern is recorded at the end of step 2 where the column has lost its strength due to the lateral loads. Also, the cracks are recorded at the end of step 3 where the axial load is applied till the axial failure of the tested column. Figs. 6 to 14 shows the cracks distributions.

4.2 Load-horizontal Displacement Relationship (Step 2 Loading)

The horizontal load versus the displacement at the level of the acting load is graphed for each specimen as shown in Figs. 15 to 19. It is clear that the horizontal response of each specimen is influenced by the amount of the axial loading applied on the specimens.

Table 1. Details of the column specimens

Column	Cross section (mm)	Height (mm)	Footing (mm)	Columns' RFT Ratio %	Columns' RFT	Stirrups	No. and types of FRP Plies
C2	250x250	1500	400x1000x400	1.08 %	6T12	5R8/m (Closed)	----
C2G1				1.08 %	6T12	5R8/m (Closed)	1 Ply GFRP
C2G2				1.08 %	6T12	5R8/m (Closed)	2 Plies GFRP
C2C1				1.08 %	6T12	5R8/m (Closed)	1 Ply CFRP
C2C2				1.08 %	6T12	5R8/m (Closed)	2Plies CFRP

Table 2. Physical properties of the FRP material

|	CFRP Fabrics	GFRP Fabrics
Product Label	Sikawrap-300C	Sikawrap-430G
Product Description	Unidirectional, woven carbon fiber	Unidirectional, woven glass fiber
Fabric length/roll	≥ 50 m	≥ 50 m
Fabric width	300/600 mm	600 mm
Density	1.82 g/cm^3	2.56 g/cm^3
Fabric design thickness	0.167 mm	0.168 mm
Tensile strength of fiber	4000 N/mm^2	2500 N/mm^2
Tensile E-modulus of fiber	230000 N/mm^2	72000 N/mm^2
Strain at break of fiber	1.7 %	2.7 %

Fig. 1. Test setup
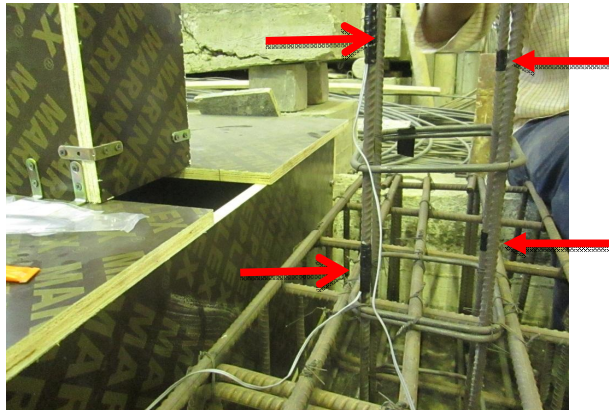
Fig. 2. Strain Gauge locations

Fig. 3. Calibration of the strain gauges

In general, the column confinement increases the ductility of the columns under the lateral loads. The increase of the number of plies slightly increases the ductility. In addition, the maximum horizontal load is measured at each cycle for the specimens during testing. Also, the axial load is maintained constant during step 2 of testing for each test. That axial load represent almost 30% of the calculated ultimate load for each column including the confinement effect. Those values are shown in Table 4.

From the above relations one can notice that the confinement of the samples has improved the ductility criteria since the lateral displacement is increased. That is shown for the specimens with 2 plies have more displacements than specimens with one ply by 18% and 29% for glass and carbon fiber consequently.

4.3 Column Axial Capacity (step 3 loading)

The horizontal repeated loads were applied on specimens till load degradation. In step 3, the horizontal loads are removed and then the axial load is increased till failure of the specimens. The maximum values of that axial load is compared with the calculated nominal value of the axial strength of such section without any lateral loads' history. That is shown in the Fig. 20. That figure shows that the axial capacity has lost about 50% of their nominal axial strength. You may notice that specimens confined with CFRP layers have the least reduction.

Table 3. Properties of the adhesive material

|	Epoxy
Product Label	Sikadur-330
Product Description	Sikadur-330 is a two-part, thixotropic epoxy based impregnating resin / adhesive
Appearance / Colors	Resin part A: Paste, Hardener part B: Paste
	Part A: white, Part B: grey
	Part A + Part B mixed: light grey
Mixing Ratio	4 (Part A): 1 (Part B)
Tensile strength	30 N/mm2
Bond strength	Concrete fracture (> 4 N/mm^2)
Tensile E-modulus	3800 N/mm^2
Strain at break of fiber	0.9 %
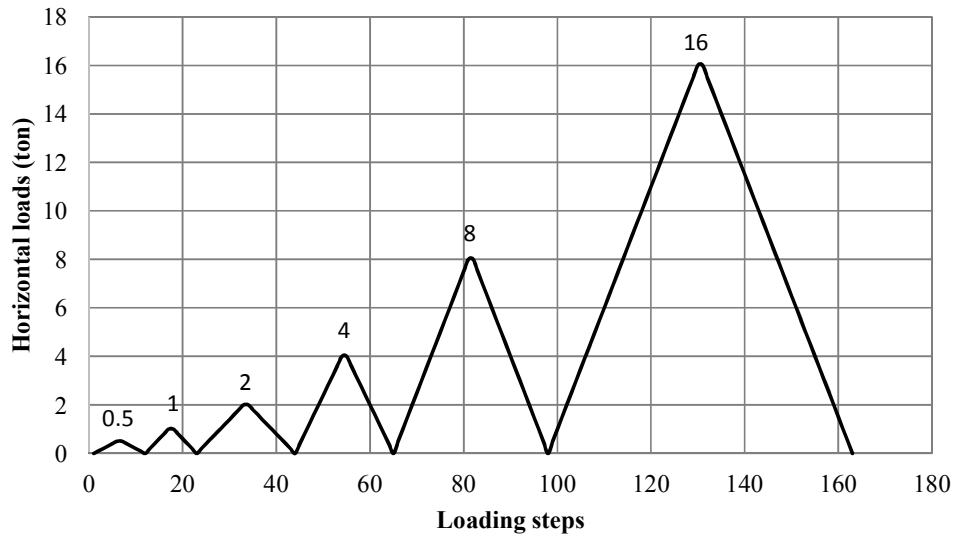
Fig. 5. The horizontal loading history plan

Fig. 6. The cracks of C2 column under the lateral loads

Fig. 7. The cracks of column c2 at failure under the ultimate axial load

Fig. 8. The cracks of column C2G2 at failure under the ultimate axial load

Fig. 9. The cracks of column C2G1 at failure under the ultimate axial load

Fig. 10. The cracks of C2G2 column at failure under the lateral load. Separation of the fiber is noticed
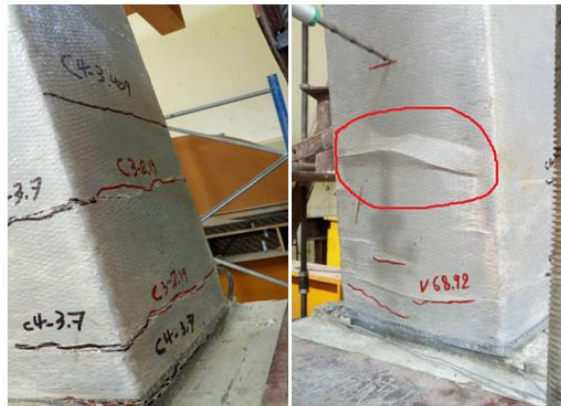

Fig. 11. The cracks of C2G1 column at failure under the lateral load. Separation of the fiber is noticed

Fig. 12. The cracks of column C2C1 at failure under the ultimate axial load

Fig. 13. The cracks of C2C1 column at failure under the lateral load. Separation of the fiber is noticed

Fig. 14. The cracks of C2C2 column at failure under the lateral load. Separation of the fiber is noticed at the marked area

Table 4. The maximum recorded horizontal load for each cycles

Specimen	Cycle 1	Cycle 2	Cycle 3	Cycle 4	Cycle 5	Cycle 6	Max Hz load	Axial app. Load (step 2)
C2	0.494	1.064	2.223	4.047	6.175	Test end	6.175	30.7
C2G1	0.503	1.024	2.19	3.7	Test end	Test end	3.700	38.5
C2G2	0.592	0.994	2.036	4.007	Test end	Test end	4.007	39.9
C2C1	0.526	1.065	2.089	4.232	8.057	8.803	8.803	43.4
C2C2	0.538	1.112	2.012	4.09	8.169	9.916	9.916	52.4
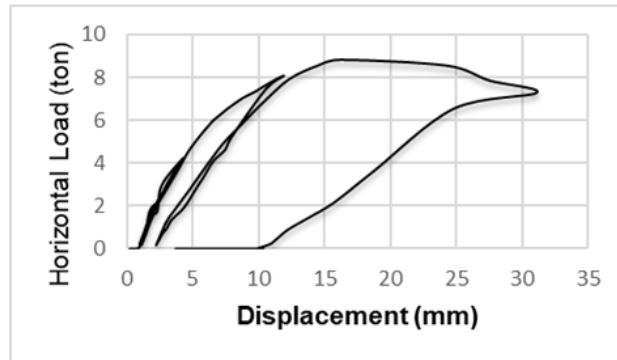
Fig. 15. The load displacement relation for C2C1
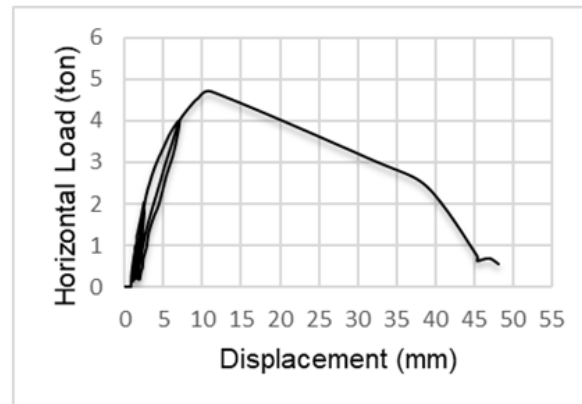
Fig. 16. The load displacement relation for C2G2
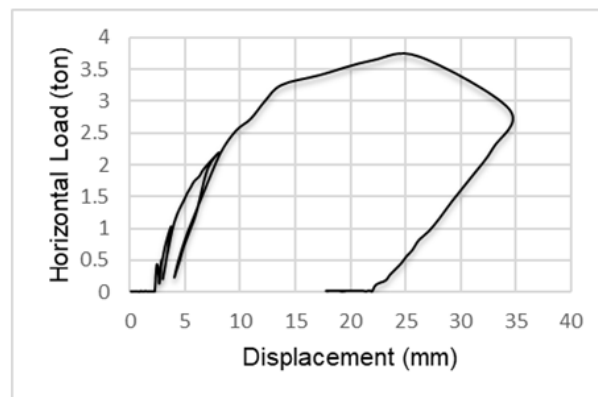
Fig. 17. The load displacement relation for C2G1
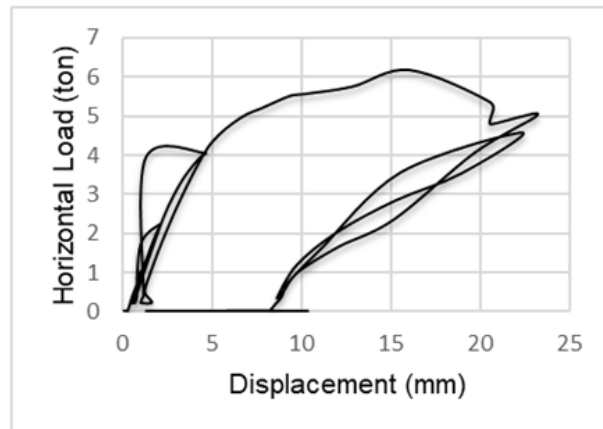
Fig. 18. The load displacement relation for C2
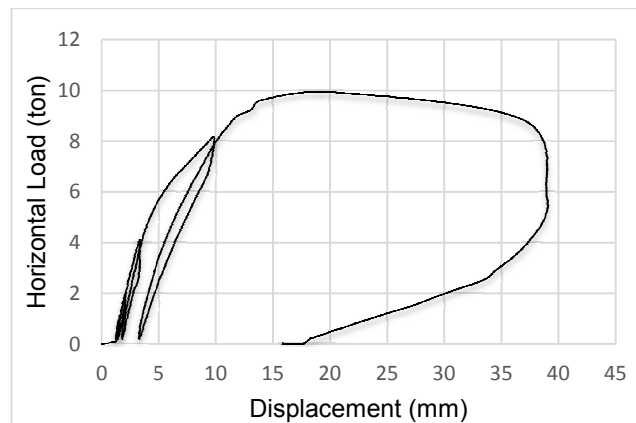
Fig. 19. The load displacement relation for C2C2
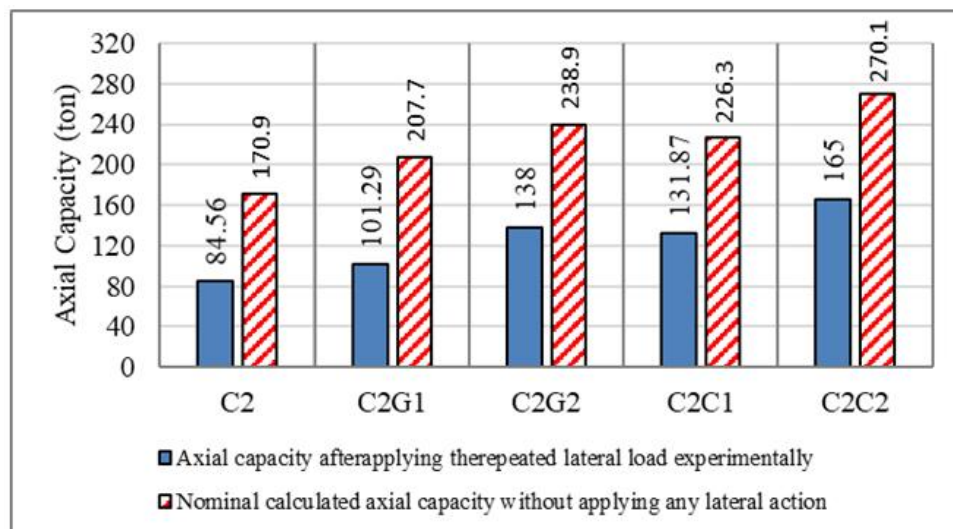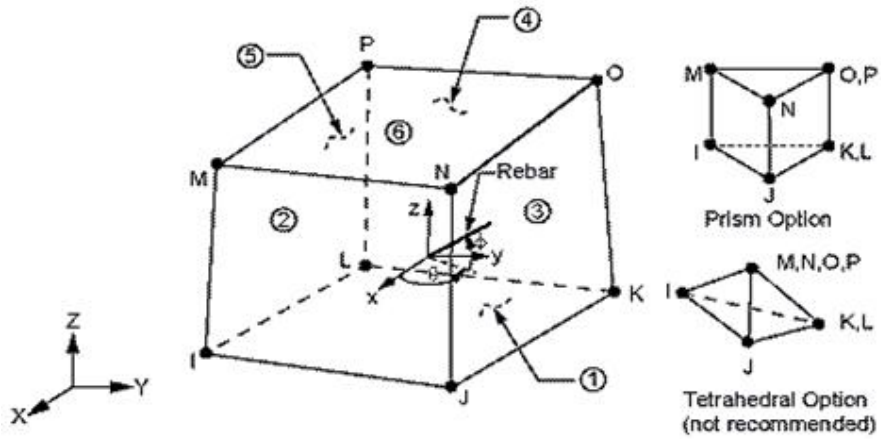
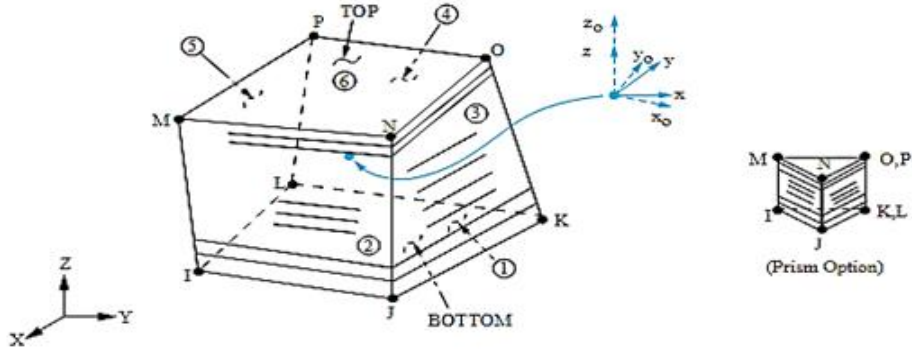

Fig. 20. Maximum axial loads after step 3 of loading

Fig. 21. Solid 65 element

x_o = Element x-axis if ESYS is not supplied.

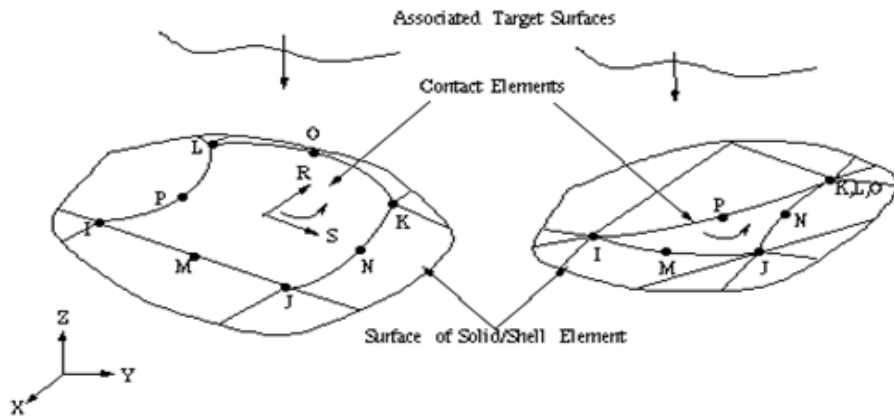x = Element x-axis if ESYS is supplied.

Fig. 22. Solid 185 element

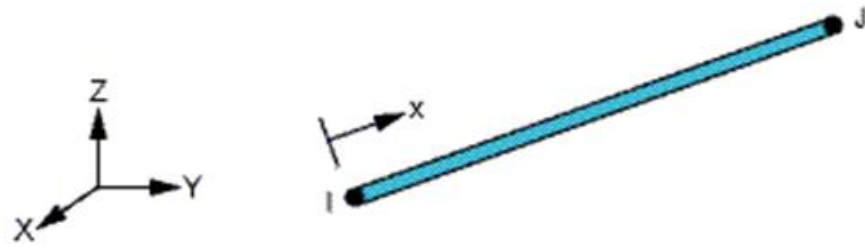**Fig. 23. CONTA173**
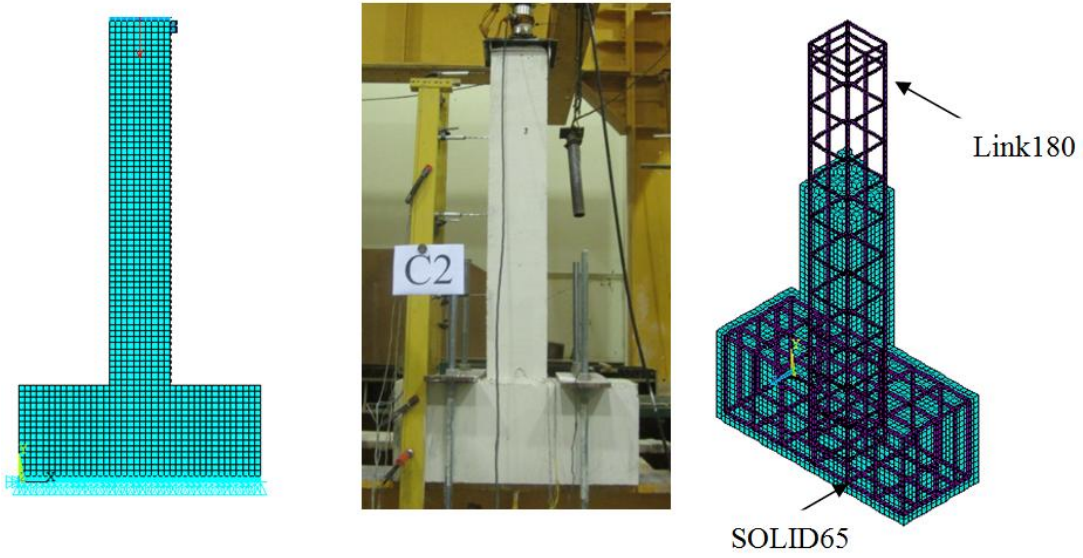
Fig. 24. Link 180 element

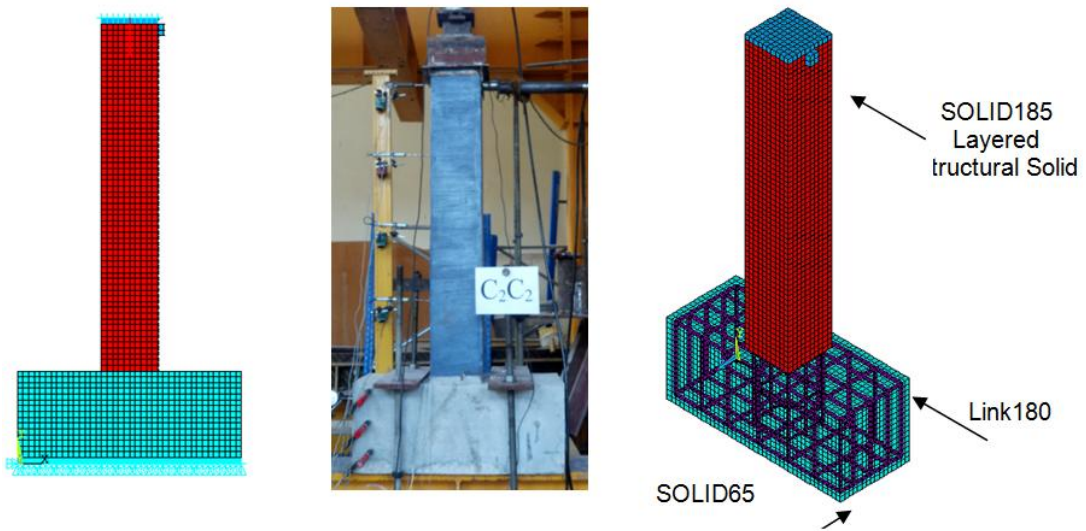**Fig. 25. Finite element model for unconfined column**

Fig. 26. Finite Element Model for confined Column

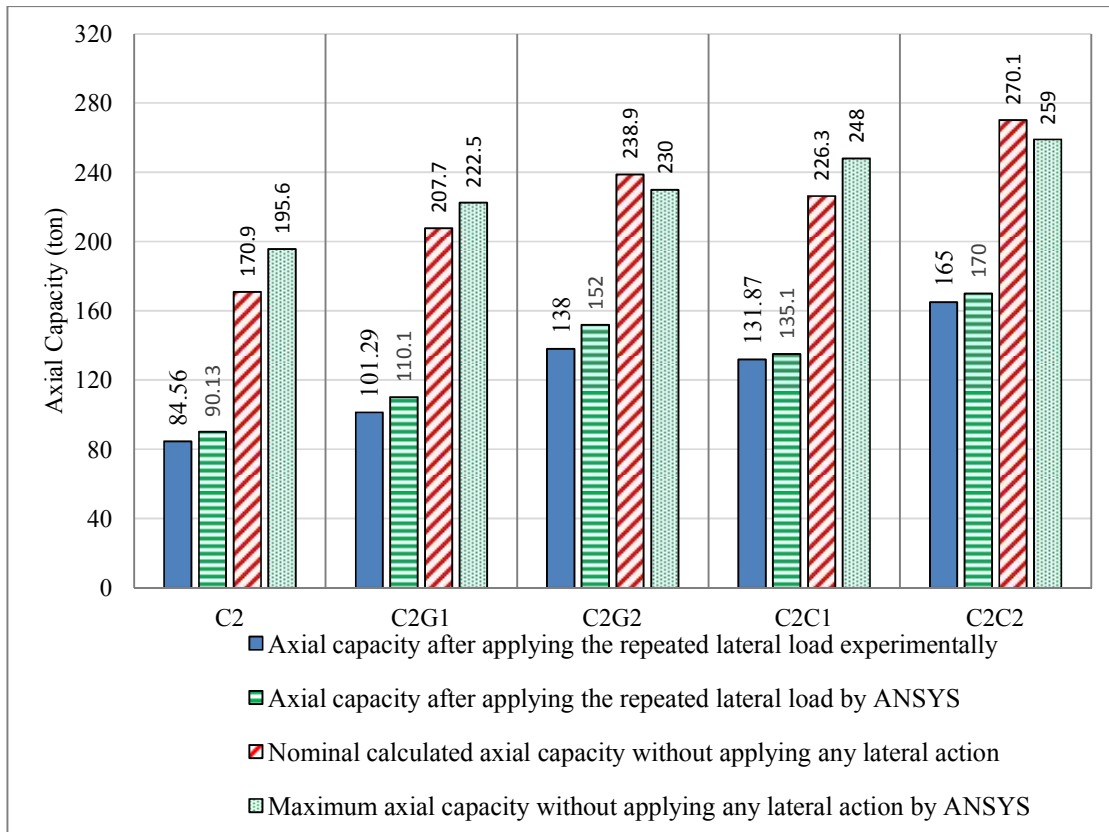**Fig. 27. Axial strength values for specimens with and without repeated horizontal loading history**
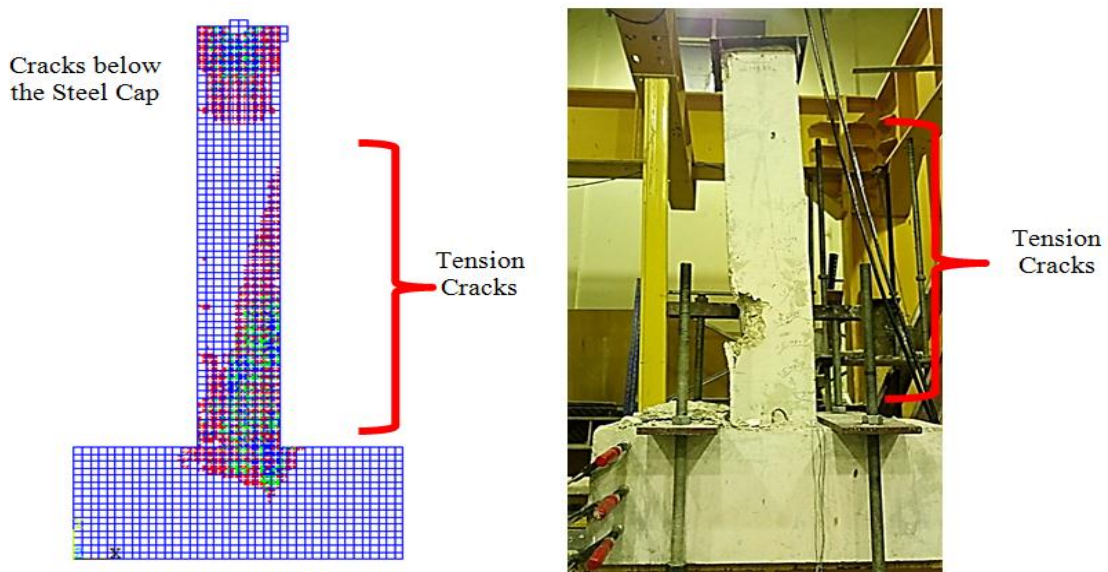
Legend:
- ■ Axial capacity after applying the repeated lateral load experimentally
- ■ Axial capacity after applying the repeated lateral load by ANSYS
- ▨ Nominal calculated axial capacity without applying any lateral action
- ▨ Maximum axial capacity without applying any lateral action by ANSYS

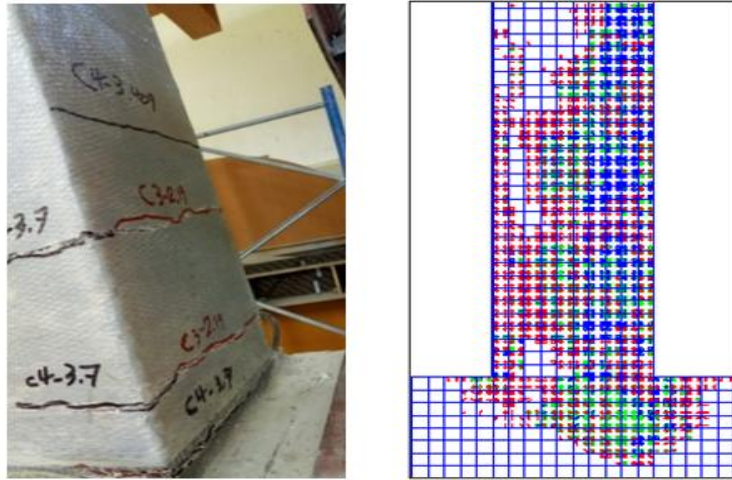**Fig. 28. Crack pattern for unconfined column**

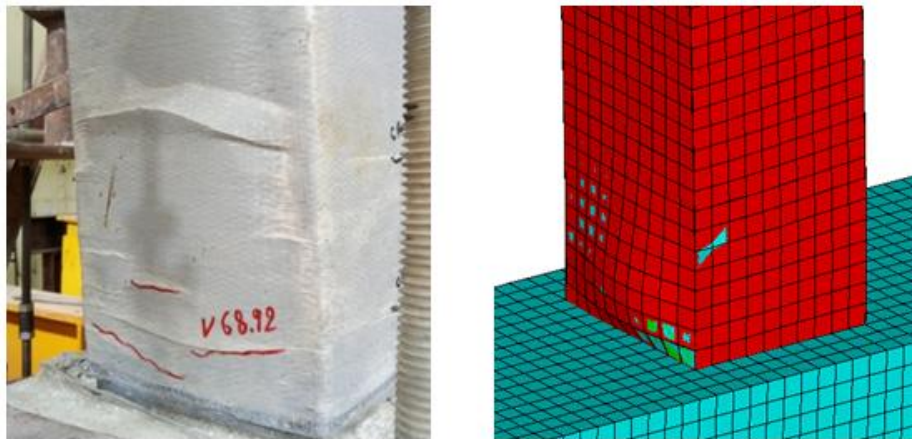**Fig. 29. Crack pattern for confined columns**

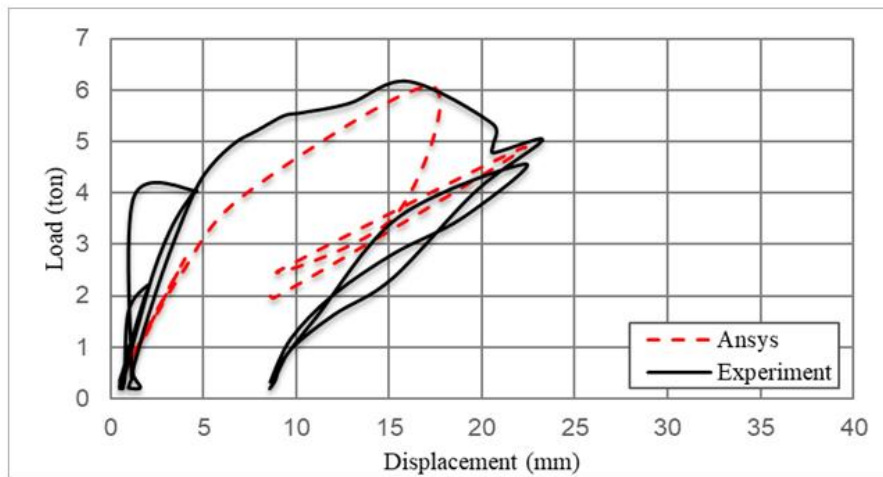**Fig. 30. Separation of FRP at the bottom of confined columns**

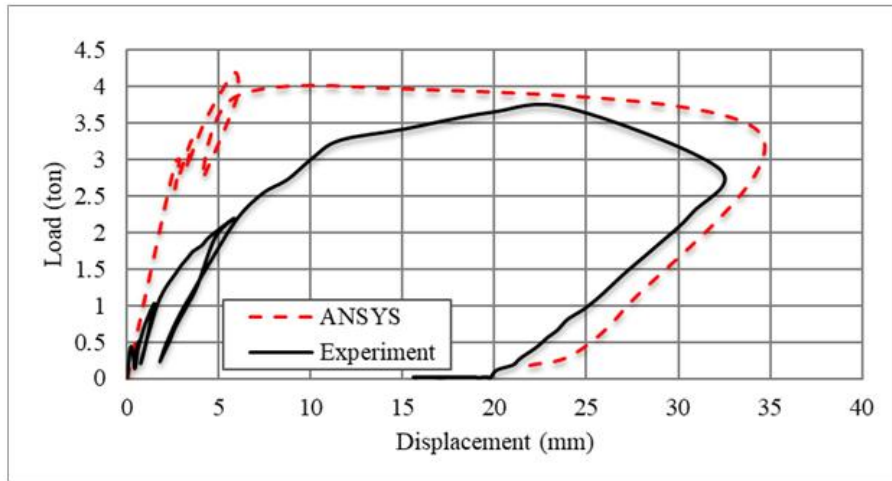**Fig. 31. Comparison for P$_h$ – Displacement Curve for C2**

Fig. 32. Comparison for P$_h$ – Displacement Curve for C2G1
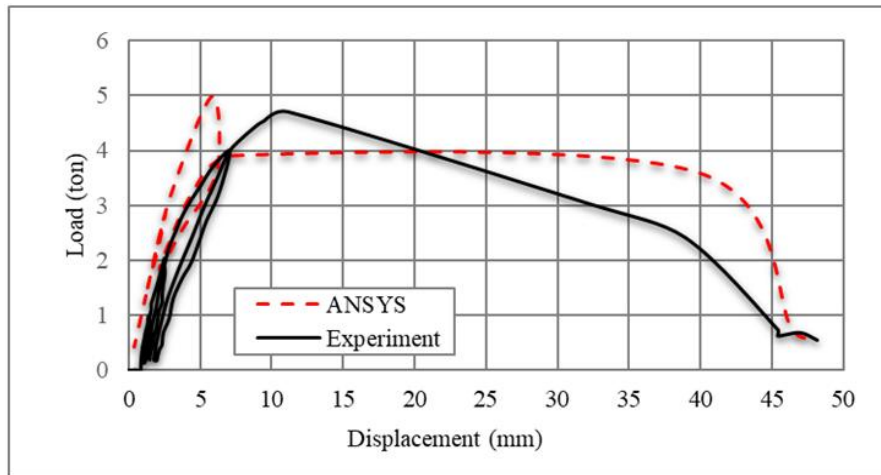

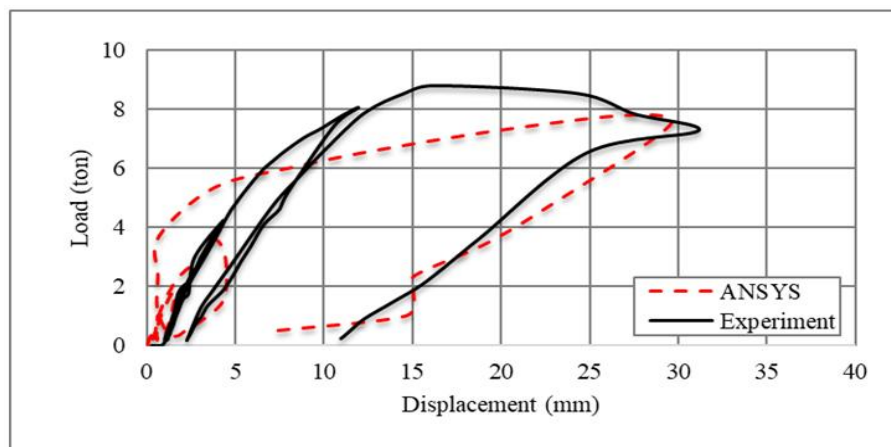**Fig. 33. Comparison for P$_h$ – Displacement Curve for C2G2**

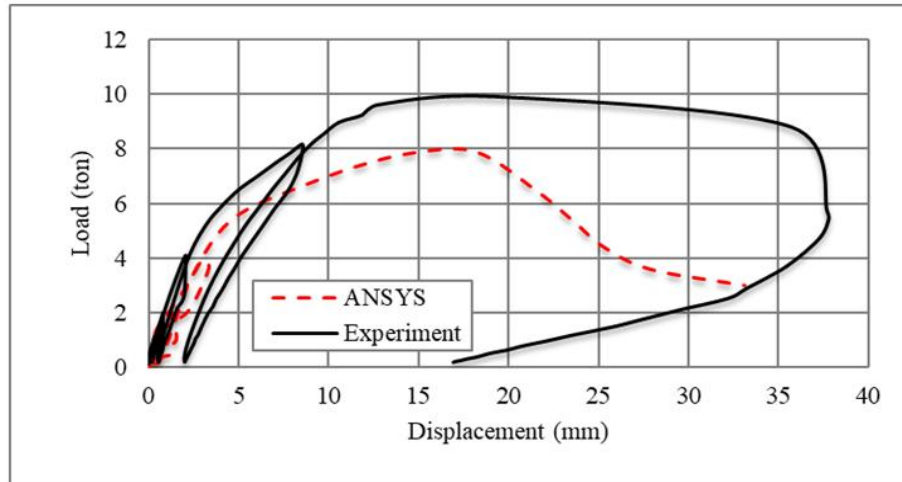**Fig. 34. Comparison for P$_h$ – Displacement Curve for C2C1**

Fig. 35. Comparison for P$_h$ – displacement curve for C2C2

5. NUMERICAL INVESTIGATION

The general purpose finite element program is utilized in our study. The experimented specimens are modeled and tested in the same procedures as they are tested. The concrete material is modelled using element SOLID 65. The element is defined by eight nodes having three degrees of freedom at each node: translations in the nodal x, y, and z directions. The solid is capable of cracking in tension and crushing in compression. The FRP material is modeled using SOLID185, see Figs. (21 to 24). In addition, the reinforcement bars are modeled using element link180. The element is defined by eight nodes having three degrees of freedom at each node: translations in the nodal x, y, and z directions. The layered composite specifications including layer thickness, material, orientation, and number of integration points through the thickness of the layer are specified via shell element. CONTA173 is used to represent contact and sliding between 3-D solid element and a deformable surface. This element has three degrees of freedom at each node: translations in the nodal x, y, and z directions. The following Figures illustrates the meshing and the reinforcement details.

6. RESULTS OF THE NUMERICAL STUDY

6.1 Lateral Strength of the Models (step 2 of loading)

The vertical loads in addition to the horizontal load history is applied to the numerical models as done for the experimented specimens. The application continue until degradation of the horizontal strength. Then after the axial load is applied till failure of the models. Table 5 shows the maximum horizontal forces for the experimented specimens and the numerical models. It is noted that the experimental results with the numerical models are in good agreement.

6.2 Axial Strength of the Models (Step 3 of Loading)

The maximum axial load is measured at failure (at the end of step 3 of loading) and presented for all specimens in the Table 6. It is noted that the experimental results with the numerical models are in good agreement. Fig. 27 shows the axial strength of specimens with lateral repeated load history. Those values are compared with the values calculated from the ANSYS model. Good agreement is found between the numerical and the experimental findings. The variation was in the range of (2%-10%) whereas the ANSYS values are always higher. Also, the maximum nominal strength for the specimens is calculated and compared with the ANSYS findings. Those values are close.

6.3 Cracking Patterns

- **Unconfined Column**

Fig. 28 illustrate the crack patterns occurred in concrete for the unconfined columns due to both lateral and axial loads. There is a match for the crack pattern found in the numerical models with the experimental outcomes all over the loading stages.

Table 5. Lateral capacities of columns from ANSYS (Ph$_{ANS}$) and experiment (Ph$_{EXP}$)

Column	Pv, Axial app. Load (step 2) (ton)	Loaded horz. till cycle no	Ph$_{ANS}$ (ton)	Ph$_{EXP}$ (ton)	Ph$_{ANS}$/Ph$_{EXP}$
C2	30.7	5	6.065	6.175	98%
C2G1	38.5	4	3.990	3.700	108%
C2G2	39.9	4	4.000	4.007	100%
C2C1	43.4	6	7.800	8.803	89%
C2C2	52.4	6	7.870	9.916	79%

Table 6. Axial capacities of columns from ANSYS (P$_{ANS}$) and experiment (P$_{EXP}$)

Column	Pv$_{ANS}$ (ton)	Pv$_{EXP}$ (ton)	Pv$_{ANS}$/Pv$_{EXP}$
C2	90.13	84.56	1.07
C2G1	110.1	101.29	1.09
C2G2	152	138	1.101
C2C1	135.1	131.87	1.02
C2C2	170	165	1.03

- **Confined Columns**

It should be noted that the crack patterns obtained from ANSYS for the confined columns is able to simulate the cracks occurred in the concrete under the FRP laminates. That is not appear on the photos taken from the experimental tests because of confinement obstruction. Therefore, the crack patterns obtained from ANSYS for the confined columns covers larger area than the experimental specimens as shown in Fig. 29.

The separation of fiber from concrete surface which is occurred in the experimental tests at the lower third of column in the compression zone. That is notice also in ANSYS models. That is due to simulating the epoxy material by contact element model as shown in Fig. 30.

6.4 Lateral Load – Displacement Curves

Comparison of the lateral-load-displacement curves for all specimens from the tests and ANSYS models are presented in the Figs. 31-35.

From the above Figures one can notice that the experimental and the numerical findings are in good agreements. Then the numerical model is valid and give a reasonable results and can be used for further studies with anther parameters.

7. CONCLUSION

1. It is found that the repeated lateral loads decrease the axial capacity of the columns with a ratio of about (38%-50%).
2. The carbon fiber achieved less reduction in the column axial capacity than the glass fiber.
3. In general, the column confinement increases the ductility of the columns under the lateral loads.
4. The increase of the number of plies slightly decreases the reduction in axial capacity due to applying repeated lateral load.
5. Good agreements are achieved between the experimental and analytical models. Simulating the epoxy material with contact element on the numerical models leads to a realistic performance for the numerical model compared with the real experimented columns.

COMPETING INTERESTS

Authors have declared that no competing interests exist.

REFERENCES

1. Shuenn-Yih Chang, Ting-Wei Chen, Ngoc-Cuong Tran, Wen-I Liao. Seismic retrofitting of RC columns with RC jackets and wing walls with different structural details, Earthquake Engineering and Engineering Vibration. 2014;13(2).
2. Hamidreza Nasersaeed. Evaluation of behavior and seismic retrofitting of RC structures by concrete jacket, Asian Journal of Applied Sciences; 2011.
3. Yeou-Fong Li, Jenn-Shin Hwang. A study of reinforced concrete bridge columns retrofitted by steel jackets, Journal of the Chinese Institute of Engineers. 2005;28(2).
4. Wang JH, Kikuchi K, Kuroki M. Seismic retrofit of existing R/C rectangular columns with circular steel jackets, 30th Conference on Our World in Concrete & Structures, Singapore; 2005.

5. Guo ZX, Liu Y, Wu YB. Experimental study on a new retrofitted scheme for seismically deficient RC columns, The 14th World Conference on Earthquake Engineering, Beijing, China; 2008.

6. Muhammad S. Memon, Shamim A. Sheikh. Seismic resistance of square concrete columns retrofitted with glass fiber-reinforced polymer. ACI Structural Journal; 2005.

7. Stathis N. Bousias, Michael N. Fardis. Experimental research on vulnerability and retrofitting of old-type RC columns under cyclic loading, Springer; 2003.

8. Hamid Saadatmanesh, Mohammad R. Ehsani, Limin. Repair of Earthquake-damaged RC columns with FRP wraps, ACI Structural Journal; 1997.

9. Mesay A. Endeshaw, Mohamed ElGawady, Ronald L. Sack, David I. McLean. Retrofit of rectangular bridge columns using CFRP wrapping Washington State Transportation Center (TRAC) - Washington State University - Department of Civil & Environmental Engineering; 2008.

10. Yan Z, Pantelides CP, Reaveley LD. Seismic retrofit of bridge columns using fiber reinforced polymer composite shells and shape modification, The 14th World Conference on Earthquake Engineering; 2008.

11. Brian J. Walkenhauer, David I. McLean. Seismic retrofit of cruciform-shaped columns in the aurora avenue bridge using FRP wrapping, Washington State University – Department of Civil & Environmental Engineering; 2010.

12. Gnanasekaran, Amlan. Seismic retrofit of columns in buildings for flexure using concrete jacket, ISET Journal of Earthquake Technology, 2009;46(2):505.

Peer-review history:
The peer review history for this paper can be accessed here:
http://www.sdiarticle3.com/review-history/50643